Journal of Sustainability Science and Management
Volume 17 Number 2, February 2022: 55-66
eISSN: 2672-7226

INHIBITORY EFFECTS OF ASTAXANTHIN ON LPS-INDUCED RAW 264.7 INFLAMMATION AND BREAST CANCER MCF-7 CELL LINES PROLIFERATION

BAYAN YOUSEF AL-TARIFI[1], AZIZAH MAHMOOD[1], HASSAN I. SHEIKH[1], WAN AMIR NIZAM WAN AHMAD[2] AND SUVIK ASSAW[2,3]*

[1]Faculty of Fisheries and Food Science, Universiti Malaysia Terengganu, 21030 Kuala Nerus, Terengganu, Malaysia. [2]School of Health Sciences, Universiti Sains Malaysia, 16150 Kubang Kerian, Kelantan, Malaysia. [3]Faculty of Science and Marine Environment, Universiti Malaysia Terengganu, 21030 Kuala Nerus, Terengganu, Malaysia.

**Corresponding author: aasuvik@umt.edu.my*
Submitted final draft: 11 January 2021 *Accepted: 18 February 2021* http://doi.org/10.46754/jssm.2022.02.006

Abstract: Astaxanthin (ASTA) is a xanthophyll carotenoid pigment derived from bacteria, yeasts, and microalgae *Hematococcus pluvialis* and is known to exhibit a potent antioxidant activity that protects the biological system against free radicals. Moreover, ASTA is also known to possess medicinal values such as anti-cancer and anti-inflammatory activities, however, the mechanism on how ASTA exhibits these properties are not well understood. The aims of this study were to elucidate the mechanism of the cytotoxic effect of ASTA on breast cancer cell line MCF-7 and its anti-inflammatory effect on monocytic RAW 264.7 cells. Cytotoxic activity of ASTA on both cells line was determined using MTT assays and further studied the anti-cancer mechanism of ASTA on MCF-7 by computational docking study. Meanwhile, the anti-inflammatory activity mechanism was elucidated on LPS induced nitric oxide (NO) production and its association with cell activation. Results revealed that ASTA had a different cytotoxic effect on breast cancer cell MCF-7 and RAW 264.7 cells. In addition, the computational docking study revealed that the anti-cancer activity of ASTA was due to significant high energy efficiency combining with estrogen receptor (-8.3) and Quinon reductase (-8.1) rather than the Janus kinase receptor (-7.4). We also demonstrated the ability of ASTA to inhibit the LPS-induced RAW 264.7 to become activated macrophages and subsequently reduced the nitric oxide production. In conclusion, ASTA exhibits its anti-inflammatory activities by affecting macrophages activation in vitro. Meanwhile, ASTA also has been demonstrated to have anti-proliferative activity by significantly reducing the MCF-7 cell viability and survivability. Computational molecular docking further revealed the anti-proliferative mechanism of ASTA, where it has a strong affinity towards ER and Quinone reductase receptors on MCF-7 but not JNK2.

Keywords: Microalgae, astaxanthin, anti-cancer, anti-inflammatory, *Hematococcus pluvialis*.

Introduction

Astaxanthin (ASTA) a natural antioxidant compound of the xanthophyll family, it plays an important role to protect the biological system against free radicals (Petrou *et al*., 2018). Recently, the use of ASTA in food, pharmaceuticals and nutraceuticals has been rapidly growing. It provides various biological advantages, including antioxidant, anti-inflammatory and anti-cancer effects in mammals. (McCall *et al*., 2018). ASTA has a unique structure consists of two terminals joined by a polyene chain, long conjugated double bonds, hydroxyl and keto groups moieties on both ends (Chen *et al.,* 2015*)*liver function, antioxidants activities and astaxanthin absorption rate were investigated. 45 hamsters were split into 5 groups and fed with normal diet, high-cholesterol control (0.2% cholesterol. Various stereoisomers of ASTA exist related to hydroxyl group configuration on the chiral carbon C-3 and C3', two enantiomers (3S,3'S) is a predominant form of natural ASTA and (3R, 3'R), while (3R, 3'S) is a mesomer isomer of ASTA (Yang *et al*., 2013).

Inflammation plays an important role in the production and progression of various diseases in different organs (Farruggia *et al*.,

2013). ASTA has been presented to inhibit TLR4 ligand lipopolysaccharide (LPS) induced systemic inflammation through inhibition of pro-inflammatory mediators by suppression of NF-κB and iNOS by inhibiting IKK activity (Takahashi *et al*., 2011). Moreover, the exposure of monocytic RAW 264.7 cell to LPS has significantly promoted the cell into activated macrophages which manifested with morphological changes and size such as having enlarged cells/nucleus along with the formation of pseudopodia and granules. These activated macrophages release several pro-inflammatory mediators including nitric oxide (NO) (Muniandy *et al*., 2018). Even though many reports have demonstrated that astaxanthin able to inhibit the LPS-induced NO production in RAW 264.7, however up to date there is a lack of reports showing its association with the ability of ASTA to delay or inhibit the activation of these cells.

In recent years, computational docking has become a powerful effective screening tool for detecting novel potential compound leads and advanced computer-based design (Yu *et al*., 2012) 2-phenylindole. Thus, different signals play a major role in tumorigenesis and are considered an important therapeutic target for a natural product. Free radicals and reactive oxygen species (ROS) are unstable atoms with an extra electron, which react quickly with molecules to initiate chain reactions, highly accumulation of free radicals that trigger oxidative damage of lipids and protein, and cellular damage (Ekpe *et al*., 2018). Increasing the level of free radical that promote cell converted into a malignant cell, this may be related to mitochondrial dysfunction (Galadari *et al*., 2017). In addition, elevated ROS levels have been associated with cancer initiation, propagation, cancer cell transformation and chemotherapy resistance (Prasad *et al*., 2017). According to previous research of ASTA against many diseases and commonly used in antioxidant prevention and treatment. ASTA has shown anti-cancer properties by inhibits tumor progression according to abrogation estrogen receptor alpha (6V87), Janus Kinase2 (JNK2) and protein Quinine reductase (4zvm) (Wang *et al*., 2013), however, the mechanism on how ASTA bind to these receptors are not clearly understood. Therefore, in this study, we further elucidated the mechanism of the cytotoxic effect of ASTA on breast cancer cell line MCF-7 and its anti-inflammatory effect on monocytic RAW 264.7 cells.

Materials and Methods

Chemicals and Reagents

ASTA powder was extracted from green microalgae (*Hematococcus pluvialis*) was purchased from BGG company in China (AztaZine®; SDHP-05) provided 5% oil. Monocytic cell lines (RAW 264.7) was obtained from American Type Culture Collection (ATCC, Manassa, VA, USA) and routinely cultured in MEM (Sigma, Lot #RNBH0274, Japan) supplemented with 10% fetal bovine serum (FBS, Sigma, BCBR07 18V, USA), 1% penicillin-streptomycin mixed solution (nacalai tesque, Japan), MTT (3-(4,5-dimethylthiazol-2-yl)-2,5-diphenyl tetrazolium bromide) (nacalai tesque, Lot# M8M8349, Japan), Griess (sigma, Lot# SLBT0574, USA), sodium nitrite ($NaNO_2$) (Sigma Aldrich, USA), DAPI (4′-6-diamidino-2-phenylindole) (Sigma, USA).

ASTA Preparation

Twenty grams of natural ASTA was dissolved in 100% dimethylsulfoxide (DMSO), the sample was centrifuged at 5000 rpm for 10 minutes at 4°C. The sample was kept at 4°C until further use.

Cells Culture

RAW 264.7 in MEM complete media was cultured, while MCF-7 in DMEM completed media were cultured. Both culture media were supplemented with 1% penicillin-streptomycin, 1% sodium pyruvate and 1% essential amino acid. The cells were treated with 1 ml of 0.25% of trypsin when the cells detached from the bottom and flask wall become clear, 3 ml of media was added into flask then suspended very

well, the media and trypsin were transferred into 15 ml centrifuge tube for 5 minutes, 20°C, 1000 rpm, after removing old media, 2 ml of new media was added and a subculture at a ratio 2:1. When the cells overgrew and become confluent the cells were collected by centrifugation, the cell cryopreservation solution as a ratio (FBS: DMSO = 7:3) for MCF-7 and (FBS: DMSO = 9:1) for RAW 264.7 cells. Both cells then were placed in a sterile cryovial and liquid nitrogen.

MTT Cytotoxic Assays

RAW 264.7 cells were grown into 96 plates for 24 hours at the density of 2×10^5 cell/ml (100 µl) before treatments. Then old media is discarded and cells treated with different ASTA concentrations (0 - 100 µg/ml) and 0.06% H_2O_2 (positive control) and 0.5% DMSO (negative control). After 24, 48, and 72 hours incubation, the cell morphology was observed and photomicrographs were taken by using an inverted microscope. Meanwhile, for MCF-7, the cells were grown in non-coated 96- well plates at the density (5×10^4 cell/ml) with medium and treatments ASTA (0-50µM) for 48 hours. Then 20 µl of MTT was added into each well and was kept for 4 hours, then old media was removed and 100 µl of DMSO was added into each well. After 10 minutes of incubation the plates were placed into a microplate reader (Thermo scientific; VARIOSKAN FLASH) to measure the absorbance in the living cells at 540 nm.

Anti-inflammatory Mechanism of ASTA

Measurement of NO Level

RAW 264.7 cells were treated with various concentrations of ASTA (0-100µg) 30 minutes before induction with 1µg/ml of LPS. Cells were cultured in an incubator at 37°C with 5% CO_2 and air relative humidity >80%. After 24 hours incubation, photomicrographs of the cell morphology from all well and cell size were taken at 20x by using an inverted microscope. Then the medium in each well was transferred into a 2 ml tube and centrifuged at 1000 rpm, 37°C for 1 minutes. Then, 100 µl aliquots of cell supernatants were added into new 96 plates and were mixed with 100 µl of Griess reagent. The plate was incubated for 20 minutes and the colour changes were measured at 540 nm by using a microplate reader (Thermo scientific; Varioskan Flash). The concentration of nitrite in the sample was determined by using the sodium nitrite (Sigma Aldrich) standard curve (25 µM – 1000 µM) (Lee *et al*., 2013) as a reference.

Cell Size

RAW 264.7 cell size were observed and quantified. In this study, RAW 264.7 cells were treated with 0.1µl LPS was activated after 24 hours. The photos were captured by using an inverted microscope at magnification 200X (1X51, OLYMPUS, Tokyo, Japan). Cell diameter was measured and quantified by using Image J-NIH software with 8 replicates for each treatment group.

DAPI (4',6-diamidino-2-phenylindole) Nuclei Staining

To further investigate the effect of ASTA on cell activation, the nucleus of activated RAW 264.7 were observed using DAPI staining. Around 5 mg DAPI was dissolved in 1 ml distilled water to obtain a 1 mg/ml stock solution. For working solution used 1:500 dilutions on the section for 10 minutes. 50 µl of DAPI solution was added to each well contains cells. Optimal vital staining required incubation for 30 minutes. The nucleus morphology was observed and determined using UV/VIS Molecule devices.

Computational Molecular Docking for an anti-cancer mechanism of ASTA on MCF-7

Ligand preparation

The molecular models of the estrogen alpha, Janus kinase 2 and protein Quinone reductase inhibitors were built with the use of Guass View software. The chemical structures of the inhibitors were provided in Figure 1. The calculation was carried out with MM2-Minimize energy with minimum RMS Gradient 0.0100 display every nth alteration. All files optimized were run saved in pdb extension.

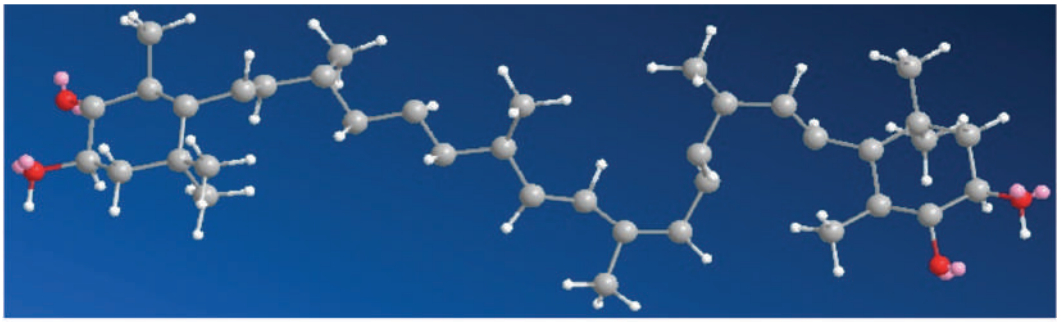

Figure 1: Chemical structure of ASTA draws by Chemdraw

Molecular Docking with Auto Dock Vina

Therefore, AutoDockTools 1.5.6 (ADT) was used to combine all non-polar hydrogen and add Gasteiger charges followed by setting up the rotatable bonds and saved in PDBQT format. Likewise, the protein estrogen alpha crystal structure (PDB ID: 6V87 1.8A; 2020), Janus kinase 2 (JNK2) and protein Quinone reductase (4Zvm; 2015) was retrieved from RCSB protein data bank (http:// www.rcsb.org.pdb). Thereafter, proteins and co-crystallized ligand were prepared as described before. Autodock Vina 1.0.2 was used to proceed with docking by using the rigid protein structure. A docking net with a size 30A×30A×30A was used. The center coordinate of the middle atom of the co-crystalized inhibitor was used for each docking. All dockings were run an 8 Intel Dual-Core 3.0 GHZ computer cluster. AutoDock Vina presents the docking scores as free of binding energy (ΔG).

Statistical analysis

All data were presented as mean ± S.E.M. The statistical analysis was performed using Graph pad Prism (version 7.01). All data were analyzed by using One Way AVOVA and Two Way ANOVA between-group where is appropriate and followed by multiple comparison post hoc test. $P<0.05$ was considered significantly different between groups.

Results and Discussion

Cytotoxic Effect of ASTA on RAW 264.7 Cell

Monocyte RAW 264.7 cell viability in the presence of ASTA at different concentrations is shown in Figure 2. The data indicate that ASTA is having differential cytotoxic effects following the exposure period. Results revealed that ASTA does not affect cell viability during 24 hours of exposure and was having a cell growth-promoting effect. The cell viability was significantly ($p<0.05$) higher at all concentrated tested when compared with the control group as shown in Figure 2. This data is in agreement with the study by Wang *et al*. (2009) which reported that ASTA (40 µM) was promoting cell growth after 24 hours incubation. Meanwhile, when the cells were further incubated with the presence of ASTA for 48 and 72 hours, the cell viability decreased significantly relative to the control group. This data indicates that prolonged exposure of ASTA to the cells can produce cytotoxic and the most suitable time to use the ASTA as treatment is recommended not more than 24 hours in any assays. Moreover, at a high concentration of ASTA the cell viability was reduced to (45%) after 48 hours incubation compared with the control group without morphological changes as shown in Figure 3. In addition, according to Nguyen *et al*. (2017) demonstrated that the cell viability decreased when the concentration of ASTA increased and treat cell up to 100 µg/ml the cell viability decreased to (50%). Increasing incubation time to 72 hours, the viability of the cells was continuously decreased with ASTA

concentration increased, while the control group showed no effects on cell viability (100.8 ± 15.4%) as shown in Figure 2. The reduction of cell viability after 72 hours may be related to increasing ASTA concentration and exposure time that cause cell shrinkage and rounding that reduce the number of cells (Wayakanon *et al*.,

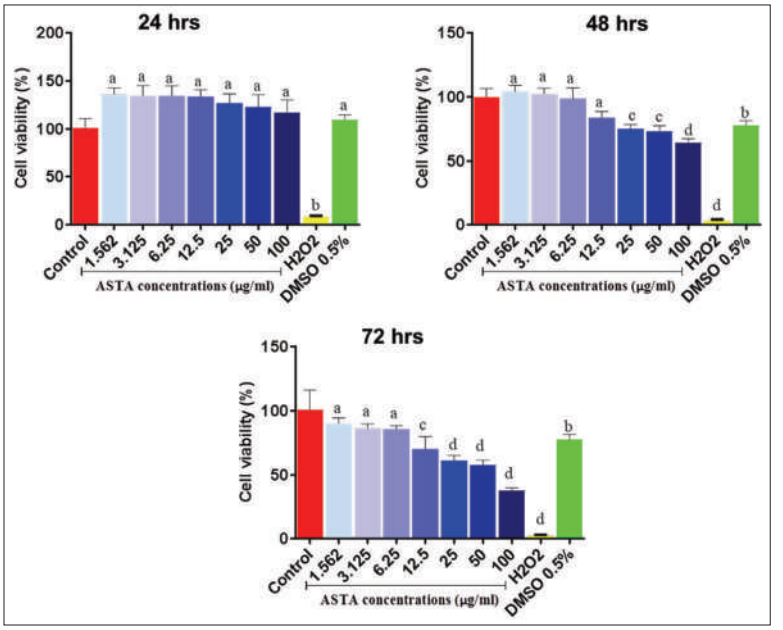

Figure 2: Cytotoxicity activity of ASTA extracted from *Hematococcus pluvialis* on RAW 264.7 cells. Cells were treated with different concentrations (0-100µg/ml) of ASTA for 24, 48 and 72 hours. The effect of ASTA on cell viability was determined by using MTT assay. Data are presented as mean values of cell viability ± SEM. $^{a}P<0.05$ $^{b}P<0.01$, $^{c}P<0.001$ & $^{d}P<0.0001$ were significantly different to the control group (n=8) analyzed using One Way ANOVA followed by Dunnett's multiple comparisons

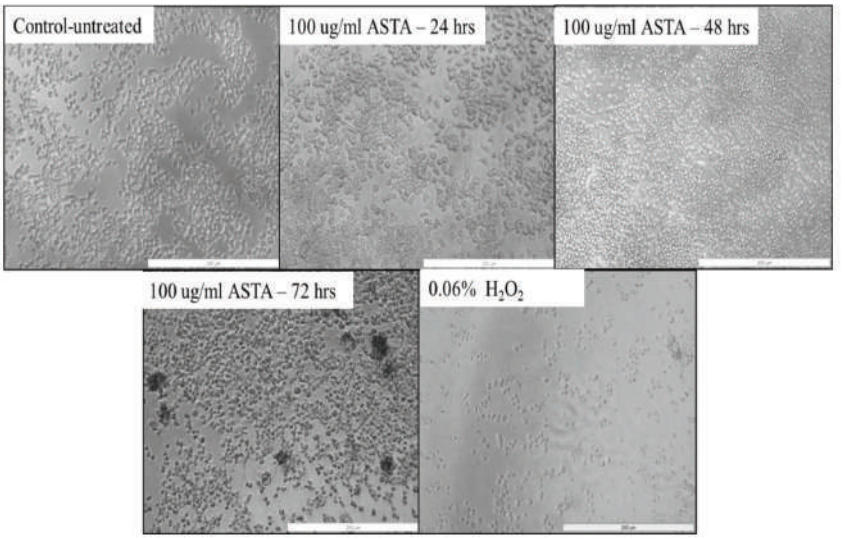

Figure 3: The effect of ASTA on RAW 264.7 cells at a different exposure time at 24, 48 and 72 hours

2018). As expected the positive control 0.06% hydrogen peroxide demolished almost all the cells in the culture at 24, 48 and 72 hours as shown in Figures 2 and 3.

Effect of ASTA on Nitric Oxide Production

ASTA was evaluated using LPS induced RAW 264.7 for *in vitro* anti-inflammatory activity. In this study, the *in vitro* anti-inflammatory assays, results showed that LPS has caused a significant ($p<0.0001$) elevation of NO in RAW 264.7 cells by almost 15 fold when compared to untreated cells (LPS treated: 15.7 ± 0.7µM vs untreated: 0.0 ± 0.0µM) as shown in Figure 4. Interestingly, pre-treatment of cells with ASTA 30 minutes prior to LPS significantly reduced the LPS-induced NO production in a dose-dependent manner with a reduction of NO level almost 57.6% in cells treated with 100µg/ml ASTA when compared to LPS-induced RAW 264.7 (Figure 4).

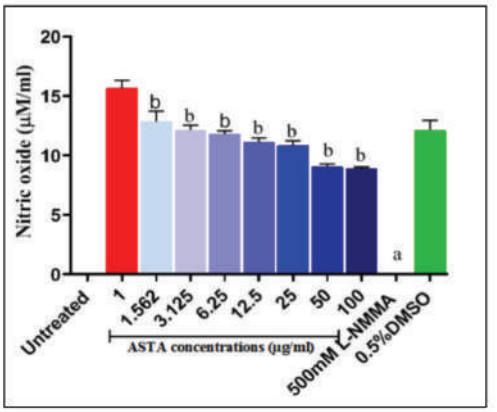

Figure 4: Anti-inflammatory effect of ASTA at different concentrations on pro-inflammatory mediator nitric oxide (NO) production in LPS-induced RAW 264.7 cells. Data are presented as mean values of nitric oxide concentration ± SEM. $^{a}P<0.05$ & $^{b}P<0.01$ were significantly different to the treated group (n=8) analyzed using One Way ANOVA followed by Dunnett's multiple comparisons

Effect of ASTA on RAW 264.7 Cell Activation

Results revealed that exposure of LPS on the RAW 264.7 has promoted the monocytic cells to become activated macrophages which manifested with the formation of pseudopodia, enlargement of the nucleus and also the irregular shape of cells morphology when compared to untreated cells which appear to be the more circular and small size as shown in Figure 5a & 5b. Moreover, the anti-inflammatory properties of ASTA are strongly suggested to be associated with its ability to inhibit cell activation which manifested by the reduction in cell size as shown in Figures 5a & 5b. At the highest concentration tested (100 µg/ml), ASTA was found to significantly ($p<0.0001$) reduced the LPS-induced cell size from the mean size of 77.1 µm to 61.5 µm. The ASTA-treated cells were also found to have a smaller nucleus, lack of pseudopodia formation and granules as shown in Figure 5b. However, the cells treated with ASTA are significantly bigger than those in the untreated cells. This further suggests that the ASTA might not only inhibiting the activation of RAW 264.7 cell into inflammatory macrophages (M1) but somehow it might also differentiate the cells into anti-inflammatory phenotype (M2) macrophages thus reducing the release of NO. As reported by Farruggia *et al*. (2018) ASTA decreased M1 polarization of bone marrow-derived macrophages (BMDM) while elevating the anti-inflammatory M2 macrophage polarization together with its ability to suppress the translocation of NF-kB translocation and pro-inflammatory genes expression. In addition, ASTA is also known to suppress the LPS induced activation of NF-kB pathways and inhibits cytokines production in vitro and in vivo (Farruggia *et al*., 2018 & Priyadarshini & Aggarwal, 2018). Furthermore, DAPI staining analyses further confirm the effect of ASTA on LPS-induced RAW 264.7, where ASTA-treated cells had smaller nucleus sizes relative to LPS-treated cells as shown in Figure 5c.

Effect of ASTA on Breast Cancer Cell Line MCF-7

In order to evaluate the effect of ASTA on breast cancer MCF-7 cell line, the cells were treated with various concentrations of ASTA (0 - 50 µM)

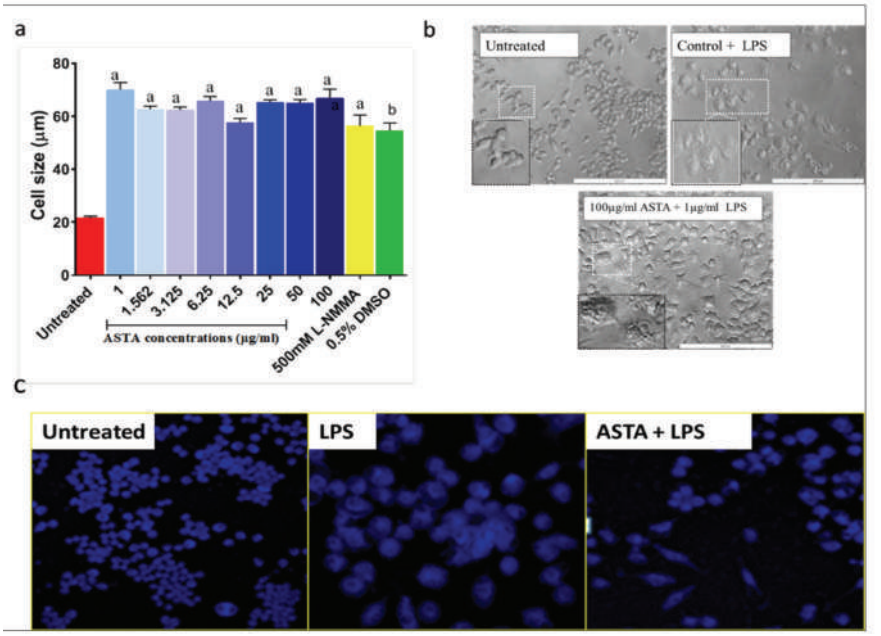

Figure 5: Effect of ASTA on the cell activation and average cell size of LPS induced RAW 264.7 cells. (a) cells morphology after 24 hours of ASTA treatment, (b) cell size of untreated cells compared to activated macrophages treated with ASTA on the differentiation RAW264.7 cell, (c) and nucleus morphology stained with DAPI staining. Data are presented as mean values of cell size ± SEM, (n=8). $^{a}P<0.0001$ & $^{b}P<0.001$ indicate significant differences from the untreated group

for 48 hours and examined the cell viability by using MTT assay. Interestingly, contradictory results with the RAW 264.7 cells, where here the ASTA had a significant anti-proliferative effect on MCF-7 in a dose-dependent manner as shown in Figure 6a. Moreover, ASTA can be a potent alternative treatment for breast cancer medication as we have demonstrated that ASTA has low toxicity on normal monocytic cells such as RAW 264.7 cell when compared to cytotoxicity on cancerous cell line MCF-7 at 24 hours of incubation as shown in Figure 6a and 6b. These findings were in agreement with Atalay *et al*. (2019) which reported a significant reduction of MCF-7 after treated with ASTA after 24 hours incubation. Furthermore, these results also in line with Régnier *et al*. (2015)a powerful antioxidant, is a good candidate for the prevention of intracellular oxidative stress. The aim of the study was to compare the antioxidant activity of astaxanthin present in two natural extracts from Haematococcus pluvialis, a microalgae strain, with that of synthetic astaxanthin. Natural extracts were obtained either by solvent or supercritical extraction methods. UV, HPLC-DAD and (HPLC-(atmospheric pressure chemical ionization (APCI which showed that the anti-cancer effect of ASTA was up to 40µM on MCF-7 and HepG2 cells. ASTA plays a major role as an anti-cancer by duel mechanism first: Increasing membrane permeability and the second mechanism by interaction with microtubules related to the blockage of the mitotic cycle (Régnier *et al*., 2015) a powerful antioxidant, is a good candidate for the prevention of intracellular oxidative stress. The aim of the study was to compare the antioxidant activity of astaxanthin present in two natural extracts from Haematococcus pluvialis, a microalgae strain, with that of synthetic astaxanthin. Natural extracts were obtained either by solvent or supercritical extraction methods. UV, HPLC-DAD and (HPLC-(atmospheric pressure chemical ionization (APCI. Other

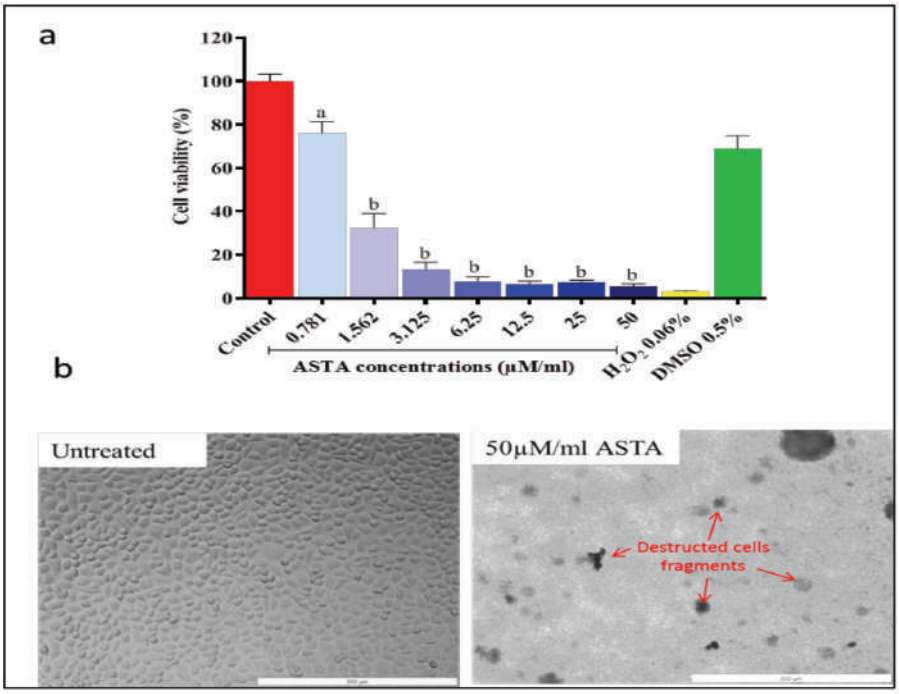

Figure 6: Cytotoxicity activity of ASTA extracted from *Hematococcus pluvialis* on breast cancer cell line MCF-7. (a) Cells were treated with different ASTA concentrations (0-50 uM) for 48 hours. ASTA 's impact on cell viability was calculated using MTT assay. Data represented mean values of cell viability ± SEM. $^{a}P<0.05$ & $^{b}P<0.01$ were significantly different to the control group (n=8) analyzed using One Way ANOVA followed by Dunnett's multiple comparisons

more increasing membrane permeability, ASTA also has been demonstrated to have an effect on apoptotic and on the proliferative pathway. Cell proliferation depends on signals transmitted by growth factors and adhesion proteins and is typically regulated by signaling cascades such as mitogen-activated protein kinase (MAPK) and phosphatidylinositide (PI3K) (Ostan *et al*., 2015). Proliferation processes and further invasion, migration, and adhesion involve actin cytoskeleton rearrangement. It includes releasing pre-existing cell-matrix contacts and establishing new integrin-substratum contacts (Zhang & Wang, 2015). Several studies have shown that ASTA exercises its antiproliferative activity through various molecules and pathways, including signal transducer and transcription activator 3 (STAT3), kappa-light-chain-enhancer nuclear factor of activated B cells (NF-µB) and gamma-activated receptor peroxisome proliferator (PPARπ) (Naji *et al*., 2019).

Computational Docking Studies on the Anti-cancer Mechanism of ASTA on MCF-7

In this study, we further elucidated the mechanism of ASTA against breast cancer cell MCF-7 by using a computational docking system on various targets of anti-cancer protein receptors on the cells namely estrogen receptor alpha (6V87), Janus Kinase 2 (JNK2) and protein Quinone reductase (4Zvm). Protein docking prognosis of the structure of protein complex of the single protein has developed significantly in these days Vakser, (2014) generally, is more difficult to determine experimentally than the structure of an individual protein. Adequate computational techniques to model protein interactions are important because of the growing number of known protein structures, particularly

in the context of structural genomics. Docking offers tools for fundamental studies of protein interactions and provides a structural basis for drug design. Protein-protein docking is the prediction of the structure of the complex, given the structures of the individual proteins. In the heart of the docking methodology is the notion of steric and physicochemical complementarity at the protein-protein interface. Originally, mostly high-resolution, experimentally determined (primarily by x-ray crystallography by embraced more adequate energy powerful and functions technique to compounds energy landscapes. Generally, ASTA structure consisted of two hydroxyl groups and is predicted to have lower potential energy inhibiting alpha-estrogen hormone. Computational docking system results revealed that ASTA was having a strong affinity to α- estrogen receptor (6V87). The affinity binding of ASTA α- estrogen receptor (6V87) was measured to be approximately (-8.3 kcal/mol). In addition, results also found that the common amino acid residues for the compound binding to α- estrogen receptor (6V87) included TYR A: 526, via conventional hydrogen bond LEU A: 387 via pi-alkyl interaction LYS A: 529, LEU A: 384 and MET A: 388 (Figure 7a). While the results performed molecule docking of ASTA with JAK2 was found to bind with JAK2 with a docking score (-8.1 kcal/mol). ASTA interacts with the dimerization site of JAK2 to form pi-Alkyl LEU A: 855 and ILE A: 1018 as shown in (Figure 7b). Meanwhile, results also revealed that ASTA has a lower affinity of ASTA binding with Protein Quinone reductase with a docking score (-7.4 kcal/mol) (Figure 7c) when compared to α- estrogen receptor (6V87) and Janus Kinase 2 (JNK2) as shown in Table 1. ASTA detection related to hydrophobicity properties, which encourage the scientist for developing new products (Varma *et al*., 2010). In another hand, the average number of hydrophobic atoms is marked in the interaction of ASTA with Estrogen receptor alpha and protein Quinone reductase. These findings mean increasing the hydrophobicity interactions can increase the binding affinity of ASTA. In addition, the presence of water molecules in the hydrophobic site makes the region more flexible. The results showed the hypothetical model of effect ASTA against human breast cancer (MCF-7) by interacting with two receptors according to trial first: Estrogen receptor alpha followed by protein Quinone reductase and Janus kinase2 respectively.

Table 1: Energy affinity of ASTA on different binding sites

Molecular Protein	Affinity (Kcal/mol)
α-estrogen protein (6V87)	-8.3
Janus kinase 2 (JACK2)	-8.1
Protein quinone reductase (4zvm)	-7.4

Conclusion

As conclusion, ASTA exhibits its anti-inflammatory activities by affecting macrophages activation in vitro. Meanwhile, ASTA has been demonstrated to have anti-proliferative activity by significantly reducing the MCF-7 cell viability and survivability. Computational molecular docking further revealed the anti-proliferative mechanism of ASTA, where it has a strong affinity towards ER and QR receptors on MCF-7 but not JNK2. The findings from this study further added to the potential use of ASTA from *Hematococcus pluvalis* in the development of alternative drugs for pharmaceutical and nutraceutical use. The findings from this study further added to the potential use of ASTA from *Hematococcus pluvalis* in the development of alternative drugs for pharmaceutical and nutraceutical use.

Acknowledgements

The authors appreciate the financial support of the Universiti Malaysia Terengganu research grant (PGRG No 55193/7) provided by Universiti Malaysia Terengganu and the Ministry of Higher Education Malaysia. We also would like to thank the Institute of Marine Biotechnology (IMB) and School of Health Science, Universiti Sains Malaysia, Kubang Kerian, Kelantan for providing the facilities.

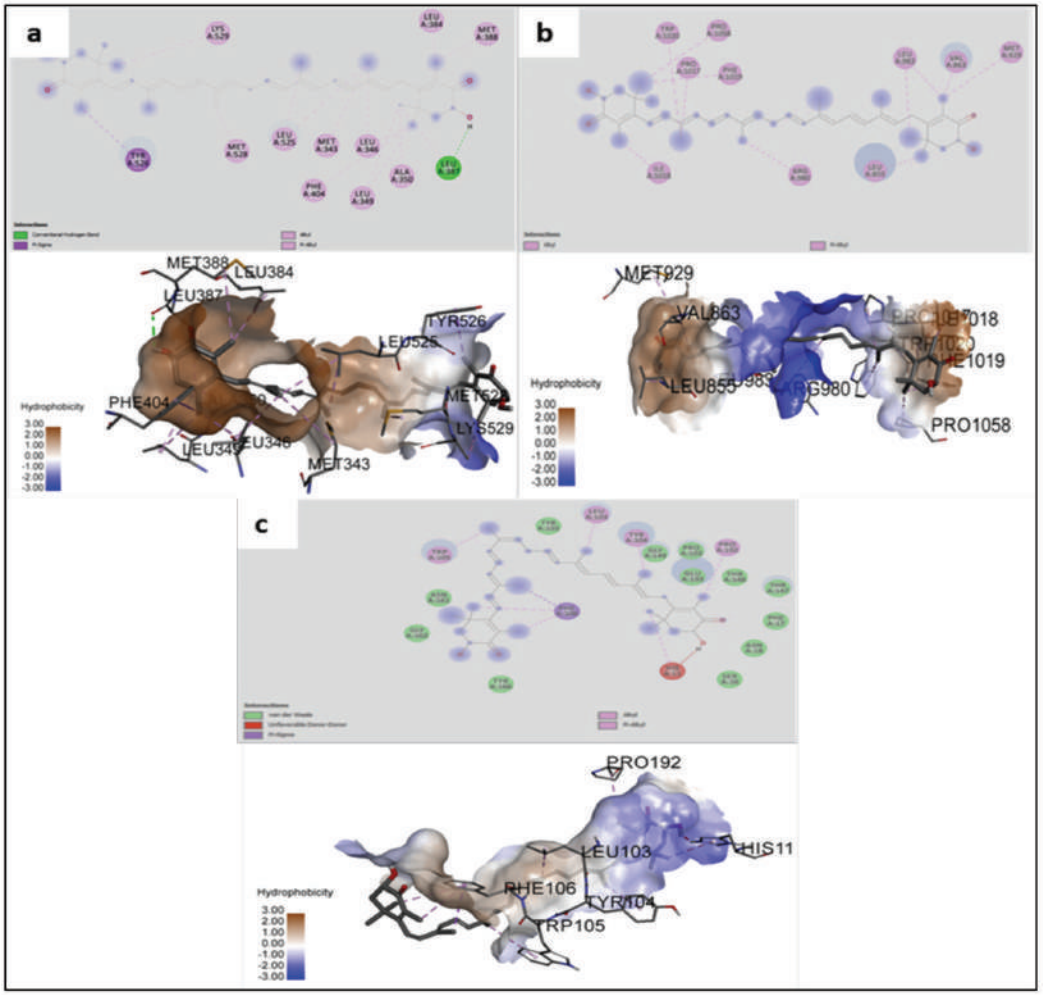

Figure 7: The ligand associated to the specific target with hydrophobic interactions inferring the biological activity of ASTA in MCF-7 receptor. (a) Hydrophobic interaction of ASTA with α- estrogen receptor (6V87), (b) Hydrophobic interaction of ASTA with Janus kinase2 (JNK2). (c) Hydrophobic interaction of ASTA with protein Quinone reductase (4Zvm)

References

Atalay, P. B., Kuku, G., & Tuna, B. G. (2019). Effects of carbendazim and astaxanthin co-treatment on the proliferation of MCF-7 breast cancer cells. *In Vitro Cellular and Developmental Biology - Animal*, *55*(2), 113-119.

Chen, Y. Y., Lee, P. C., Wu, Y. L., & Liu, L. Y. (2015). In vivo effects of free form astaxanthin powder on anti-oxidation and lipid metabolism with high-cholesterol diet. *PLoS ONE*, *10*(8), 1-16.

Ekpe, L., Inaku, K. O., & Ekpe, V. (2018). Antioxidant effects of astaxanthin in various diseases-a review. *Journal of Molecular Pathophysiology*, *7*(1), 1-6.

Farruggia, C., Kim, M. B., Bae, M., Lee, Y., Pham, T. X., Yang, Y., ... & Lee, J. Y. (2018). Astaxanthin exerts anti-inflammatory and antioxidant effects in macrophages

in NRF2-dependent and independent manners. *The Journal of Nutritional Biochemistry*, *62*, 202-209.

Galadari, S., Rahman, A., Pallichankandy, S., & Thayyullathil, F. (2017). Reactive oxygen species and cancer paradox: To promote or to suppress? *Free Radical Biology and Medicine*, *104*(8), 144-164.

Lee, S. Y., Kim, H. J., & Han, J. S. (2013). Anti-inflammatory effect of oyster shell extract in LPS-stimulated Raw 264.7 cells. *Preventive Nutrition and Food Science*, *18*(1), 23.

McCall, B., McPartland, C. K., Moore, R., Frank-Kamenetskii, A., & Booth, B. W. (2018). Effects of astaxanthin on the proliferation and migration of breast cancer cells in vitro. *Antioxidants*, *7*(10).

Muniandy, K., Gothai, S., Badran, K. M., Suresh Kumar, S., Esa, N. M., & Arulselvan, P. (2018). Suppression of proinflammatory cytokines and mediators in LPS-induced RAW 264.7 macrophages by stem extract of alternanthera sessilis via the inhibition of the NF-κB pathway. *Journal of Immunology Research*, *2018*.

Naji, T., Niazi, S., & Hamedani, P. S. K. (2019). The cytotoxic effects of astaxanthin on breast cancer cells. In *Proceedings of the International Conference on BioMedical Sciences (ICBMS19), Istanbul, Turkey* (pp. 27-28).

Nguyen, V. P., Kim, S. W., Kim, H., Kim, H., Seok, K. H., Jung, M. J., … Kang, H. W. (2017). Biocompatible astaxanthin as a novel marineoriented agent for dual chemo-photothermal therapy. *PLoS ONE*, *12*(4), 1-23.

Ostan, R., Lanzarini, C., Pini, E., Scurti, M., Vianello, D., Bertarelli, C., ... & Martucci, M. (2015). Inflammaging and cancer: A challenge for the Mediterranean diet. *Nutrients*, *7*(4), 2589-2621.

Petrou, A. L., Petrou, P. L., Ntanos, T., & Liapis, A. (2018). A possible role for singlet oxygen in the degradation of various antioxidants. A meta-analysis and review of literature data. *Antioxidants*, *7*(3), 1-32.

Prasad, S., Gupta, S. C., & Tyagi, A. K. (2017). Reactive oxygen species (ROS) and cancer: Role of antioxidative nutraceuticals. *Cancer Letters*, *387*, 95-105.

Priyadarshini, L., & Aggarwal, A. (2018). Astaxanthin inhibits cytokines production and inflammatory gene expression by suppressing IκB kinase-dependent nuclear factor κB activation in pre and postpartum Murrah buffaloes during different seasons. *Veterinary World*, *11*(6), 782.

Régnier, P., Bastias, J., Rodriguez-Ruiz, V., Caballero-Casero, N., Caballo, C., Sicilia, D., … Pavon-Djavid, G. (2015). Astaxanthin from Haematococcus pluvialis prevents oxidative stress on human endothelial cells without toxicity. *Marine Drugs*, *13*(5), 2857-2874.

Takahashi, K., Takimoto, T., Sato, K., & Akiba, Y. (2011). Effect of dietary supplementation of astaxanthin from Phaffia rhodozyma on lipopolysaccharide-induced early inflammatory responses in male broiler chickens (Gallus gallus) fed a corn-enriched diet. *Animal Science Journal*, *82*(6), 753-758.

Tarnowski, B. I., Spinale, F. G., & Nicholson, J. H. (1991). DAPI as a useful stain for nuclear quantitation. *Biotechnic and Histochemistry*, *66*(6), 296-302.

Wang, M., Zhang, J., Song, X., Liu, W., Zhang, L., Wang, X., & Lv, C. (2013). Astaxanthin ameliorates lung fibrosis in vivo and in vitro by preventing transdifferentiation, inhibiting proliferation, and promoting apoptosis of activated cells. *Food and Chemical Toxicology*, *56*, 450-458.

Vakser, I. A. (2014). Protein-protein docking: From interaction to interactome. *Biophysical Journal*, *107*(8), 1785-1793.

Varma, A. K., Patil, R., Das, S., Stanley, A., Yadav, L., & Sudhakar, A. (2010). Optimized hydrophobic interactions and

hydrogen bonding at the target-ligand interface leads the pathways of Drug-Designing. *PLoS ONE*, *5*(8), 1-10.

Wang, X., Ma, J., Bai, X., Yan, H., Qin, C., & Ren, D. (2019). Food and bioproducts processing antioxidant properties of astaxanthin produced by cofermentation between Spirulina platensis and recombinant Saccharomyces cerevisiae against mouse macrophage RAW 264 . 7 damaged by H 2 O 2. *Food and Bioproducts Processing*, *118*(35), 318-325.

Wayakanon, K., Rueangyotchanthana, K., Wayakanon, P., & Suwannachart, C. (2018). The inhibition of caco-2 proliferation by astaxanthin from xanthophyllomyces dendrorhous. *Journal of Medical Microbiology*, *67*(4), 507-513.

Wu, P., Cai, Z., Chen, J., Zhang, H., & Cai, C. (2011). Electrochemical measurement of the flux of hydrogen peroxide releasing from RAW 264.7 macrophage cells based on enzyme-attapulgite clay nanohybrids. *Biosensors and Bioelectronics*, *26*(10), 4012-4017.

Yang, Y., Kim, B., & Lee, J. (2013). Astaxanthin structure, metabolism, and health benefits. *J. Hum. Nutr. Food Sci*, *1*(1003), 1-1003.

Yu, X., Park, E. J., Kondratyuk, T. P., Pezzuto, J. M., & Sun, D. (2012). Synthesis of 2-arylindole derivatives and evaluation as nitric oxide synthase and NFκB inhibitors. *Organic and Biomolecular Chemistry*, *10*(44), 8835-8847.

Zhang, L., & Wang, H. (2015). Multiple mechanisms of anti-cancer effects exerted by astaxanthin. *Marine Drugs*, *13*(7), 4310-4330.